



ELSEVIER

Available online at [www.sciencedirect.com](http://www.sciencedirect.com)

SCIENCE @ DIRECT®

Nuclear Instruments and Methods in Physics Research A 496 (2003) 465–480

**NUCLEAR  
INSTRUMENTS  
& METHODS  
IN PHYSICS  
RESEARCH**  
Section A[www.elsevier.com/locate/nima](http://www.elsevier.com/locate/nima)

# Analog multivariate counting analyzers

Alexei V. Nikitin<sup>a,\*</sup>, Ruslan L. Davidchack<sup>a,2</sup>, Thomas P. Armstrong<sup>b,3</sup><sup>a</sup> Avatekh LLC, 2124 Vermont Street, Lawrence, KS 66046, USA<sup>b</sup> Fundamental Technologies LLC, Lawrence, KS 66046, USA

Received 20 April 2002; received in revised form 20 August 2002; accepted 1 September 2002

## Abstract

Characterizing rates of occurrence of various features of a signal is of great importance in numerous types of physical measurements. Such signal features can be defined as certain discrete coincidence events, e.g. crossings of a signal with a given threshold, or occurrence of extrema of a certain amplitude. We describe measuring rates of such events by means of analog multivariate counting analyzers. Given a continuous scalar or multicomponent (vector) input signal, an analog counting analyzer outputs a continuous signal with the instantaneous magnitude equal to the rate of occurrence of certain coincidence events. The analog nature of the proposed analyzers allows us to reformulate many problems of the traditional counting measurements, and cast them in a form which is readily addressed by methods of differential calculus rather than by algebraic or logical means of digital signal processing.

Analog counting analyzers can be easily implemented in discrete or integrated electronic circuits, do not suffer from dead time effects, and allow substantial reduction of pileup effects. Besides extending the scope of counting measurements, analog multivariate counting analyzers allow simple feedback adjustment of the parameters of the acquisition system for optimal performance. In addition, such analyzers can be made simpler, cheaper, lighter, more reliable, more accurate, and less power consuming than digital counting detectors, and thus would be ideally suited for operation in autonomous conditions such as mobile communication, space missions, prosthetic devices, etc. Other obvious immediate applications of the presented analyzers are pulse-height measuring systems used in the acquisition of nuclear radiation spectra.

© 2002 Elsevier Science B.V. All rights reserved.

PACS: 06.30.-k; 07.05.Hd; 07.05.Rm; 07.50.Ek; 29.40.-n

**Keywords:** Analog counting analyzers; Analog signal processing; Counting rates; Crossing rates; Non-linear filters; Pileup and dead time effects

## 1. Introduction

A so-called *counting detector* as defined in [1,2]<sup>4</sup> provides a basis for pulse-height analysis in

\*Corresponding author.

E-mail address: [nikitin@avatekh.com](mailto:nikitin@avatekh.com) (A.V. Nikitin).

<sup>1</sup>Also with Department of Physics, Baker University, Baldwin, KS 66006, USA.

<sup>2</sup>Also with Department of Mathematics and Computer Science, University of Leicester, University Rd., Leicester, LE1 7RH, UK.

<sup>3</sup>Also with Department of Physics and Astronomy, University of Kansas, Lawrence, KS 66045, USA.

<sup>4</sup>In the context of nuclear instrumentation, the term 'detector' is usually reserved for a device which converts radiation to an electrical signal of some sort. Here this term is used for any device converting an event into a single pulse of prespecified area.

systems for acquisition of nuclear radiation spectra [3–5]. An idealized mathematical model for such a detector is equivalent to a problem of counting the crossings of some threshold  $D$  by a continuous signal  $x(t)$ . Even though such an idealized model might seem convenient for theoretical analysis and ‘mental experimentation’, it does not correctly represent real physical measurements. Indeed, this model requires exact localization of crossings in both the amplitude and the time, that is, an infinite amplitude and time resolution. In reality, however, measurements with infinite precision are unavailable. All physical observations are limited to a finite resolving power, and the only measurable quantities are the weighted means over non-zero intervals.

On the one hand, the exact mathematical treatment of the threshold crossing problem requires usage of discontinuous and singular functions such as the Heaviside unit step function and the Dirac  $\delta$ -function [1,2]. On the other hand, as a simple consequence of inertial properties of a physical system, there are no physically realizable systems with responses described by these functions. Thus, straightforward attempts to reproduce an ideal counting system in hardware devices face various technical difficulties. Indeed, a realistic hardware implementation of a counting detector is always a trade-off between the amplitude and time resolution [6–8].

In practice, the attempts to increase both the amplitude and time resolution lead to the escalation of circuit complexity. This in turn increases the cost, weight, and power consumption of the equipment, while decreasing its reliability. Regardless of the magnitude of the technical efforts, the resulting acquisition systems will still suffer from the pileup and dead time effects.

The instrumentation for the acquisition of radiation spectra has traditionally been predicated on the assumption that the signal consists of nice clean pulses which are well separated and rise from (and return to) a solid reference level or *baseline*. Departures from these ideal conditions, such as an irregularly moving baseline and the partial superimposition of pulses, have been dealt with on a more or less ad hoc basis, with the development of gated baseline restorers, pileup rejectors and other

specialized hardware tricks to circumvent the problems [9–13]. Almost every one of these ‘band-aid’ solutions has introduced an associated problem which was not there in the first place, and ultimately all of them have been essentially brute force attempts to modify the signal and force it to behave according to the criteria required by the design of conventional systems.

Thus, in the traditional approach to pulse-height analysis, the counting problem is first reduced to an idealized mathematical model. Then, this idealized problem is addressed by non-ideal means, thus creating a variety of technical difficulties. These, in turn, are considered in terms of idealized models, breeding new technical complications. We present here a re-formulation of the initial problem in mathematical terms easily reproducible in physical devices, which remedies many of the shortcomings of the usual approaches to the counting measurements.

Our approach is to recognize the non-ideal nature of a measured signal and devise an analog processor designed to deal with such problems as shifting baseline and changing count rate, by using a real-time self-adaptive strategy. In the development of the mathematical underpinnings which follow, the threshold  $D$ , for example, is treated as a variable—not a constant. It is also recognized that whatever device is used as the threshold discriminator, it will never have the perfect and unambiguous properties which the use of  $\delta$ -functions and Heaviside step functions assumes. A practical device will have finite resolution, hysteresis, time lag, and other non-ideal properties. Accordingly, after the basic mathematical principles have been presented, non-ideal functions which emulate the essential properties of the real-world threshold discriminators are introduced to replace the discontinuous functions. These can be modeled with software to provide predictions of their performance. Some results of this modeling are presented in the subsequent sections.

## 2. Measuring threshold crossing rates by an analog circuit

In a technical sense, measurement is the process of assigning numbers or other symbols as values of

a variable, in order to establish its relation to a standard unit or to another variable of the same nature. One of the most basic ways to establish such a relation is to compare the signal  $x(t)$  with a *threshold*, or *displacement*, variable  $D$ . In practice, this can be accomplished by means of *discriminators*. An *ideal* discriminator outputs ‘0’ or ‘1’ depending on whether the signal value is larger or smaller than  $D$ , respectively. Mathematically, the output of such an ideal discriminator can be conveniently represented by the Heaviside unit step function  $\theta[D - x(t)]$ . The approach to counting described later in this paper arises out of this basic model of conducting measurements by means of discriminators.

The rate of crossings of the threshold  $D$  by a continuous signal  $x(t)$  in the time interval  $0 \leq t \leq T$  can be written as [2]<sup>5</sup>

$$\begin{aligned} \mathcal{R}(D) &= \frac{1}{T} \int_0^T dt \left| \frac{\partial}{\partial t} \theta[D - x(t)] \right| \\ &= \frac{1}{T} \int_0^T dt |\dot{x}(t)| \delta[D - x(t)] \end{aligned} \quad (1)$$

where  $\theta$  is the Heaviside unit step function,  $|\dot{x}|$  is the absolute value of the signal’s derivative, and  $\delta$  is the Dirac  $\delta$ -function.<sup>6</sup> As illustrated in Fig. 1, Eq. (1) represents measurement of threshold crossing rates by means of an ideal discriminator. Indeed, counting the number of intersections of  $x(t)$  with  $D$  (Fig. 1(a)) is equivalent to counting the number of switches of the output of the discriminator  $\theta[D - x(t)]$  between ‘0’ and ‘1’ (Fig. 1(b)). The latter counting can be performed by integrating the absolute value of the time derivative of  $\theta[D - x(t)]$  over the total time interval (Fig. 1(c)).

Replacing the rectangular weighting function in Eq. (1) by an arbitrary moving window  $w$  (normalized so that  $\int_{-\infty}^{\infty} ds w(s) = 1$ ),<sup>7</sup> the rate of crossing of the threshold  $D$  by the signal  $x(t)$  can be written

as the convolution integral

$$\begin{aligned} \mathcal{R}(D, t) &= \int_{-\infty}^{\infty} ds w(t-s) |\dot{x}(s)| \delta[D - x(s)] \\ &\equiv w(t) * \{|\dot{x}(t)| \delta[D - x(t)]\} \end{aligned} \quad (2)$$

where the asterisk denotes convolution, and the expression in the curly brackets can be interpreted as the *instantaneous* crossing rate. The modification of Eq. (2) for the rates of *upward* (+) and *downward* (–) crossings, separately, is obvious:

$$\mathcal{R}_{\pm}(D, t) = w(t) * \{|\dot{x}(t)| \theta[\pm \dot{x}(t)] \delta[D - x(t)]\}. \quad (3)$$

One might raise an objection that Eqs. (2) and (3) are hardly suitable for determining the counting rates in practice. First, these equations contain the time derivative of the signal. Second, their integrands employ a generalized function (the Dirac  $\delta$ -function) which cannot be directly evaluated.

The fact that Eqs. (2) and (3) contain the derivative of the signal  $x(t)$ , something which is not a trivial problem to measure in real time with digital techniques, does not pose a problem in the analog domain. Since physical sensors—as well as various other components of an acquisition system—have certain inertia, they have continuous time responses (typically exponential). This means that the output signal is a convolution integral of the input signal with these impulse responses, and that intermediate signals will be available before and after some stage or stages of integration. It is then a simple matter to obtain the derivative of the output signal as the real-time difference between these intermediate signals.

Consider, for example, a signal  $x_1(t)$  passing through an  $RC$ -integrator as shown in Fig. 2, where  $R_1 C_1 = \tau_1$ . Then the relation between the input signal  $x_1(t)$  and the output  $x(t)$  is given by

$$x(t) = h_{\tau_1}(t) * x_1(t) \quad (4)$$

where

$$h_{\tau_1}(t) = \theta(t) \frac{1}{\tau_1} e^{-t/\tau_1}. \quad (5)$$

Taking the derivative of  $h_{\tau_1}(t)$  leads to the following formula:

$$\begin{aligned} \dot{h}_{\tau_1}(t) &= \delta(t) \frac{1}{\tau_1} e^{-t/\tau_1} - \theta(t) \frac{1}{\tau_1^2} e^{-t/\tau_1} \\ &= \frac{1}{\tau_1} [\delta(t) - h_{\tau_1}(t)] \end{aligned} \quad (6)$$

<sup>5</sup> Derivation of Eq. (1) is also given in Appendix A.

<sup>6</sup> The Heaviside unit step function and the Dirac  $\delta$ -function are related as  $d\theta(x)/dx = \delta(x)$  [14].

<sup>7</sup> The relationship between time averaging with a weighting function  $w(t)$  and the boxcar averaging is discussed in the next section.

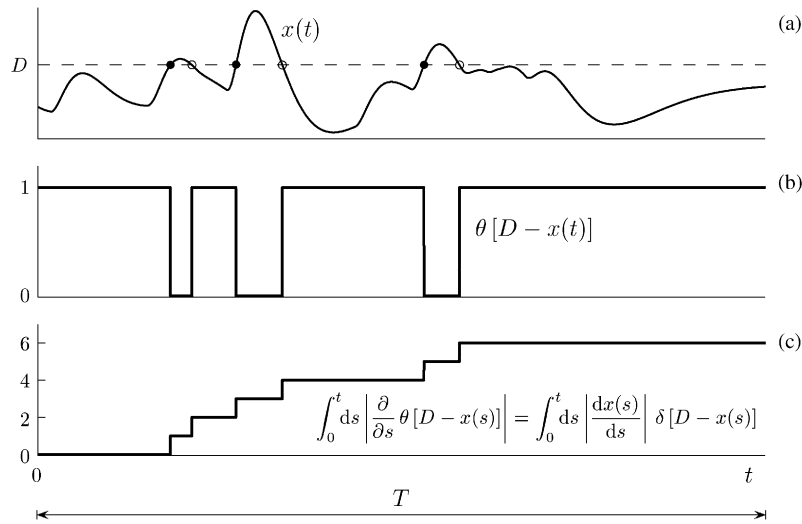


Fig. 1. Using an ideal discriminator for counting threshold crossings in the time interval  $0 \leq t \leq T$ .

where we have used the relation  $d\theta(t)/dt = \delta(t)$  and the fact that  $f(t)\delta(t) = f(0)\delta(t)$  (see [14] for example). Then the time derivative of a signal satisfying Eq. (4) can be written as

$$\dot{x}(t) = \dot{h}_{\tau_1}(t) * x_1(t) = \frac{1}{\tau_1} [x_1(t) - x(t)] \quad (7)$$

which, upon substitution into Eq. (2), leads to the following formula for computing the counting rates:

$$\mathcal{R}(D, t) = \frac{1}{\tau_1} w(t) * \{|x_1(t) - x(t)| \delta[D - x(t)]\}. \quad (8)$$

Let us emphasize that Eq. (7) expresses the time derivative of the *measured* (output) signal  $x(t)$  rather than the ‘intermediate’ signal  $x_1(t)$ . Thus we do not try to differentiate the signal by *introducing* any additional circuitry, which would result in alteration of the signal. We simply acknowledge the fact that a typical physical device already contains inertial elements, and thus time derivatives of the output can be accurately measured by ‘stepping back’ across such elements and constructing linear combinations of the intermediate signals. For example, by differentiating  $x(t)$  according to Eq. (7) we actually *restore* the high-frequency components of the signal lost on the integrator. Note also that the time derivative of

$x(t)$  can also be expressed as

$$\dot{x}(t) = h_{\tau_1}(t) * \dot{x}_1(t) = \frac{1}{\tau_2} h_{\tau_1}(t) * [x_2(t) - x_1(t)] \quad (9)$$

where  $\tau_2 = R_2 C_2$ , and the choice between using Eq. (7) or (9) should be governed by practical considerations—for example, by the values of  $\tau_1$  and  $\tau_2$ .

Eq. (8) gives an *exact* expression for the threshold crossing rates in a moving window  $w$ . This expression represents measurement of these rates with an *ideal* probe<sup>8</sup> having the response described by the  $\delta$ -function. The presence of this singular function is the second concern about practical suitability of Eqs. (2) and (3), since the integrand in Eq. (8) cannot be directly evaluated. We cannot avoid evaluating the  $\delta$ -function of the threshold argument in Eq. (8) by reverting to the time argument, since then, as should be obvious from Eq. (A.1), we would need to know the instances  $t_i$  of *all* threshold crossings, while the unavailability of these instances prompted us to convert the argument of the  $\delta$ -function from time to threshold in the first place.

<sup>8</sup>We find it convenient to use the term ‘probe’, instead of ‘differential discriminator’, for the threshold derivative of the discriminator.

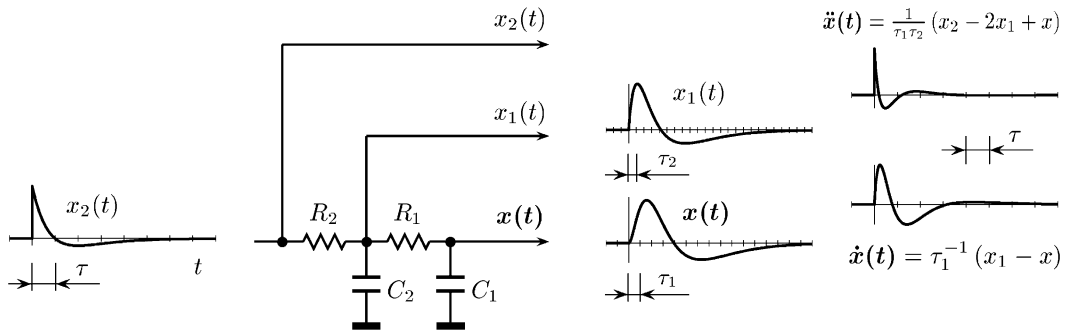


Fig. 2. Obtaining time derivatives of the output signal  $x(t)$  as the real-time difference between intermediate signals.

It is important to realize, however, that this difficulty is not inherent in our approach. Rather, it is the result of the approximation we adopted when considering the measurement process that employs an *ideal* discriminator, capable of comparison with infinite precision. In practice, the comparison of the signal with the threshold is limited to a finite resolving power, and the only measurable quantities are the weighted means over non-zero intervals. Thus, a more realistic representation of the probe would be in terms of a continuous function  $f_{\Delta D}(D)$ , which represents a *real* physical instrument [15]. Replacing the Dirac  $\delta$ -function in Eq. (8) by a finite-width probe  $f_{\Delta D}$  such that  $\int_{-\infty}^{\infty} dD f_{\Delta D}(D) = 1$ , we can re-write this equation in a form suitable for practical implementation as

$$\mathcal{R}(D, t) = \frac{1}{\tau} w(t) * \{|x_1(t) - x(t)| f_{\Delta D}[D - x(t)]\}. \quad (10)$$

The exact shape of the function  $f_{\Delta D}(D)$  in Eq. (10) will depend on the properties of the acquisition system, but will typically have a pronounced maximum around  $D = 0$  and decay to zero as  $|D| \rightarrow \infty$ . An obvious physical meaning of the width parameter  $\Delta D$  of the probe is the *amplitude resolution* of a pulse-height analyzing system employing rate counting according to Eq. (10). Another illustrative interpretation of the width parameter  $\Delta D$  can be given in terms of *fractional*, or *partial*, counts as follows. A *full* count is registered when the signal  $x(t)$  completely crosses the  $\pm \Delta D$  vicinity of the threshold  $D$ . A *partial* count is registered when the signal crosses only a

fraction of the  $\pm \Delta D$  vicinity of  $D$ . Note that such an interpretation most closely corresponds to counting with a *boxcar* probe (test function)  $f_{\Delta D}(D) = (1/2\Delta D)[\theta(D + \Delta D) - \theta(D - \Delta D)]$ , even though different types of test functions follow this interpretation in a ‘fuzzy’ fashion. Regardless of the shape of the test function, however, the partial counts become the exact counts in the limit  $\Delta D \rightarrow 0$ .

Fig. 3 illustrates two typical situations leading to partial counts (single local extrema and riding waves), and the results of counting the crossings in these situations with boxcar and Gaussian test functions. In this figure, the number of crossings is equal to the shaded areas under the instantaneous rate curves  $|\dot{x}| f_{\Delta D}(D - x)$ . Notice that, for the counts in the vicinity of an extremum, instead of a ‘jump’ from zero to two counts, the number of counts changes monotonically from zero to two over a range of threshold values of order  $\Delta D$ . This can be interpreted simply as a consequence of an uncertainty in determining the exact value of the signal at its extremum. Likewise, for the counts in the vicinity of a single riding wave, the number of counts changes monotonically from one to three over a similar range of threshold values.

A more accurate representation of real counting measurements is the main advantage of using finite-width probes for mathematical description of the counting process, which leads to a variety of efficient approaches to these measurements. In addition, employing finite-width probes for counting threshold crossings also allows significant reduction of uncertainty in counts caused by the

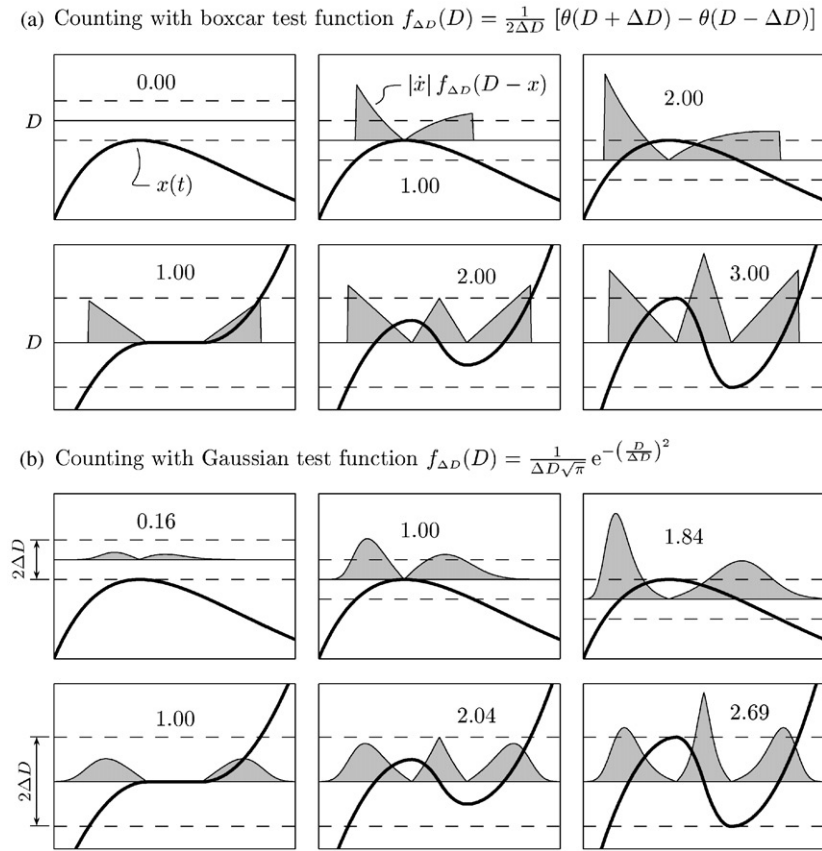


Fig. 3. Illustration of two typical situations leading to partial counts and the results of counting the crossings in these situations with boxcar and Gaussian test functions.

presence of noise, especially for ‘slow’ crossings (that is, when the absolute value of the signal’s derivative at the threshold is small). Indeed, a device implementing Eq. (10) will measure the counting rates as the weighted threshold averages with the test function  $f_{\Delta D}$ . Thus, distortions of the signal caused by fluctuations (such as, for example, the thermal noise) much smaller than  $\Delta D$  will not significantly affect the measured rates.

It is important to note that when a *continuous* probe is employed for counting measurements, the counts are no longer registered as individual events, but rather as a continuum. Indeed, when both functions  $w(t)$  and  $f_{\Delta D}(D)$  in Eq. (10) are continuous, the rate  $\mathcal{R}(D, t)$  itself is a continuous function of both time and threshold. Thus, Eq. (10) can be interpreted as an analog *signal-*

*to-rate converter*. In other words, given a continuous input signal  $x(t)$ , and a threshold  $D$ , a device implementing this equation outputs a continuous signal of the instantaneous magnitude equal to the rate of crossings of the input signal with the threshold.

One of many advantages of an analog rather than digital representation of the counting rates is that such an analog signal can be easily used as feedback in various control systems. For example, it can be used for adaptation of the parameters of the acquisition system (such as the width parameter of the probe  $\Delta D$  and/or the duration of the time weighting function  $w$ ) for the optimal compromise between the amplitude and the time resolution. For instance, it might be desirable to increase the width of  $w(t)$  in the case of low

counting rates so that the total number of counts within this window remains large. This would allow significant reduction of the statistical uncertainty in the measurements. If a digital record of the counting rates is desired (e.g., for storage or numerical output), it can simply be obtained by sampling  $\mathcal{R}(D, t)$ , that is, through a standard analog-to-digital converter.

Fig. 4 provides an example of employing Eq. (10) for measuring the rates of crossings of the signal  $x(t)$  with the threshold  $D$ . The signal represents a pulse train (such as, for instance, a train of charged particles) registered by a detector

with a time impulse response  $h(t)$  of a so-called doubly differentiated pulse, of a shape shown in Fig. 2 as  $x(t)$ . Panels 1a and b show the signal (solid lines), the threshold (horizontal dashed lines), and the width parameter  $\Delta D$  of the probe (ticks on the vertical axes, e.g., the left-hand side axis in Panel 1b). The time ticks indicate the instances of the crossings in the exact sense. Panels 2a and b show the instantaneous rates computed as the expression in the curly brackets of Eq. (10). Now each crossing results in a peak in the instantaneous rates. Note that even though the modal heights of these peaks are different,

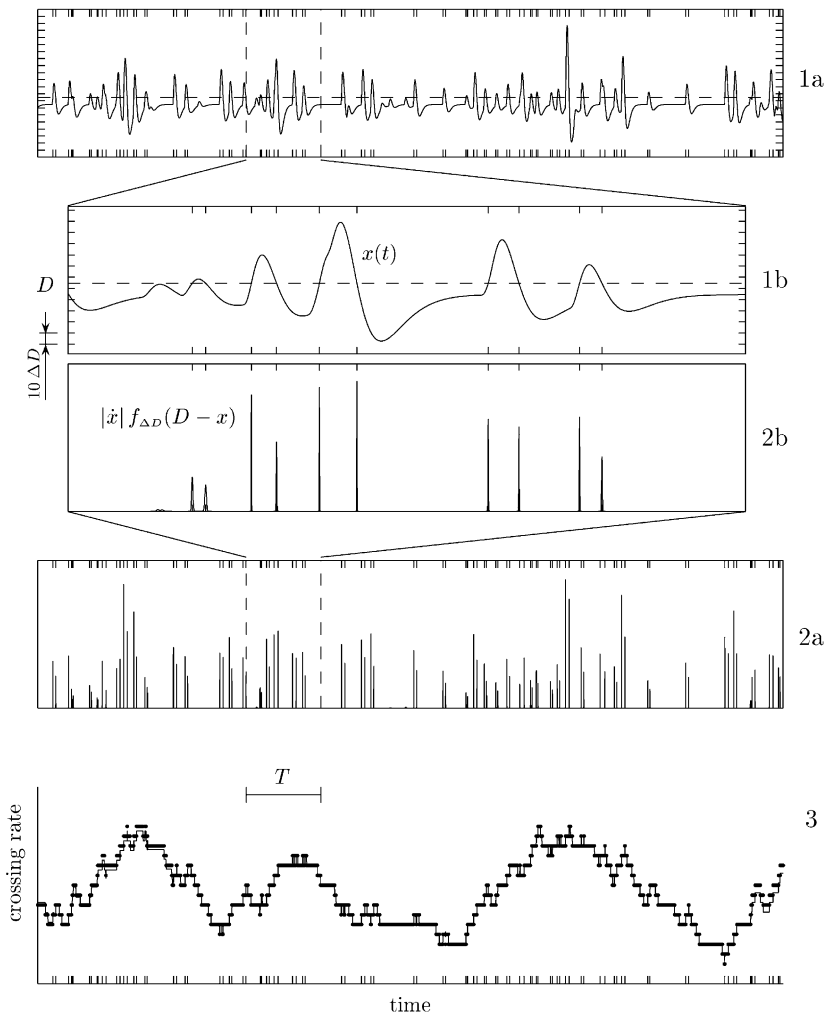


Fig. 4. Example of employing Eq. (10) for measuring the rates of crossings of the signal  $x(t)$  with the threshold  $D$ .

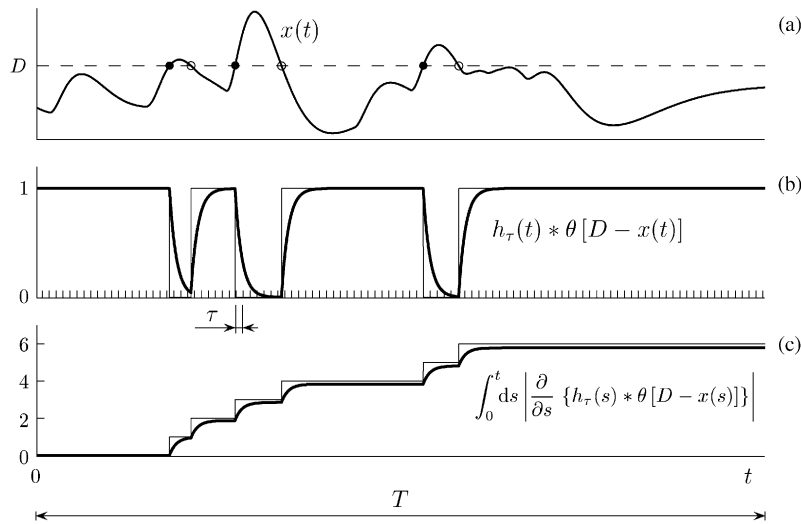


Fig. 5. Counting threshold crossings in the time interval  $0 \leq t \leq T$  by a 'slow' discriminator with an exponential time response  $h_\tau(t)$  (compare with Fig. 1).

the *integral* intensities of the peaks (that is, the areas under them) are unity. Thus time averaging of the instantaneous rates with some moving window  $w$  will result in the crossing rates within this window. Panel 3 displays the counting rates averaged with a boxcar moving window of width  $T$ . The solid line plots the rate measured through Eq. (10), and the dots correspond to the 'exact' counting rate (Eq. (8)).

### 2.1. Rate measurements with 'slow' discriminators: dead time

In our treatment of threshold crossing measurements we have assumed that the main 'imperfection' of a real discriminator was due to its finite amplitude rather than time resolution. That is, we have assumed that a discriminator has negligible inertia and changes its state between '0' and '1' immediately upon its argument inverting the sign. However, the finite time response of a discriminator might be a dominating factor in some real-life devices. Then the total response of a discriminator might be modeled as a convolution of its time impulse response  $h(t)$  with the response of an ideal discriminator  $\theta[D - x(t)]$ , and measuring threshold crossing rates with such an 'accurate

but slow' discriminator can be represented as

$$\begin{aligned} \mathcal{R}(D, t) &= w(t) * \left| \frac{\partial}{\partial t} \{h(t) * \theta[D - x(t)]\} \right| \\ &= w(t) * |\dot{h}(t) * \theta[D - x(t)]|. \end{aligned} \quad (11)$$

For instance, if the discriminator's time response is due to a single *RC*-integrator,  $h(t) = h_\tau(t)$  (see Eq. (5)), then Eq. (11) becomes

$$\begin{aligned} \mathcal{R}(D, t) &= \frac{1}{\tau} w(t) * |\theta[D - x(t)] \\ &\quad - h_\tau(t) * \theta[D - x(t)]|. \end{aligned} \quad (12)$$

Fig. 5 illustrates counting threshold crossings with such a discriminator in comparison with the counting by an ideal discriminator shown in Fig. 1.

Fig. 6 provides an example of measuring the rates of crossings of the signal  $x(t)$  with the threshold  $D$  by a slow discriminator with the exponential time impulse response  $h_\tau(t)$ , according to Eq. (12). Panels 1a and b are equivalent to those shown in Fig. 4. Panels 2a and b show the instantaneous crossing rates computed as the absolute value of the time derivative of the output of the discriminator  $h_\tau(t) * \theta[D - x(t)]$ . A *single* crossing leads to an exponentially decaying pulse of unit area in the instantaneous rates. As follows from the triangle inequality, however, the total

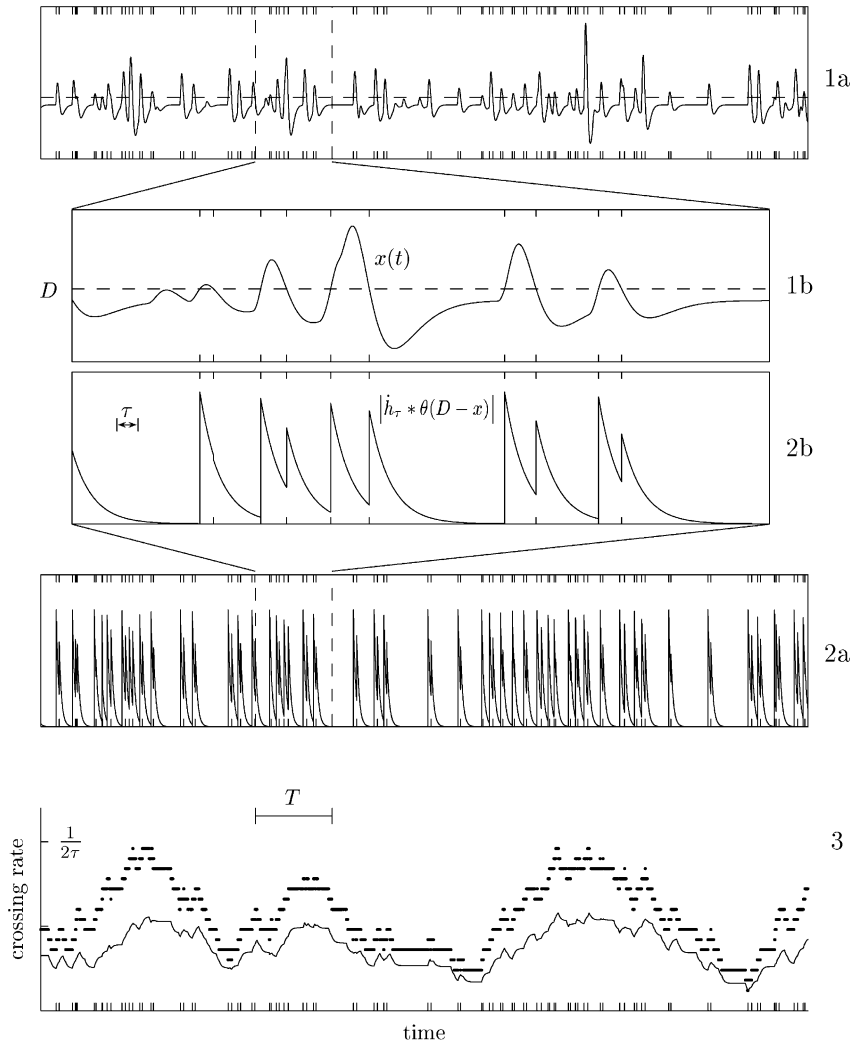


Fig. 6. Example of measuring the rates of crossings of the signal  $x(t)$  with the threshold  $D$  by a slow discriminator with the exponential time impulse response  $h_\tau(t)$ .

area under a *sequence* of such pulses is smaller than the number of crossings. Thus, a finite time resolution of the discriminator effectively results in the *dead time*, which leads to the loss of counts as illustrated in Panel 3. In this panel, the solid line plots the rate measured according to Eq. (12), and the dots correspond to the ‘exact’ counting rate given by Eq. (8).

Counting with slow discriminators leads not only to lost counts due to dead time, but also prevents us from extending the formalism of this

section to the conditional and vector rate measurements described in Section 4. Thus it will not be further discussed in this article.

### 3. Time averaging with a continuous kernel

In the example of Fig. 4 we used a boxcar moving window for time averaging of the instantaneous rates. This boxcar weighting function was used only for the ease of interpretation and for

comparison with the ‘simple’ rate (number of events per time interval). In reality, Eq. (10) represents measurement of counting rates using time averaging with the actual time impulse response  $w(t)$  of the instrument, whatever this response happens to be. Thus, even though detailed analysis of the weighted time averaging is beyond the scope of this article and some readers might find it trivial, some brief discussion of counting with a non-rectangular window is in order.

Although there is effectively no difference between averaging window functions which rise from zero to a peak and then fall again, boxcar averaging is deeply engraved in modern engineering, partially due to the ease of interpretation and numerical computations. Thus, one of the requirements for counting with a non-boxcar window is that the results of such measurements are comparable with boxcar counting.

As an example, let us consider averaging of the instantaneous rates shown in Panel 2a of Fig. 4 by a sequence of  $n$  RC-integrators. For simplicity, let us assume that these integrators have identical time constants  $\tau = RC$ , and thus their combined impulse response is

$$w_n(t) = \frac{t^{n-1}}{(n-1)!\tau^n} e^{-t/\tau} \theta(t). \quad (13)$$

Comparability with a boxcar function of width  $T$  can be achieved by equating the first two moments of the respective weighting functions. Thus, a sequence of  $n$  RC-integrators with identical time constants  $\tau = \frac{1}{2}T/\sqrt{3n}$  will provide us with rate measurements corresponding to the time averaging with a rectangular moving window of width  $T$ .<sup>9</sup>

Fig. 7 compares the rates measured with the boxcar (thin solid line) and the ‘triple-integrator’ test function ( $n = 3$  in Eq. (13), thick line) with  $\tau = T/6$ . The respective test functions are shown in the upper left corner of the figure. The gray band in the figure outlines the error interval in the rate measurements as the square root of the total number of counts in the time interval  $T$  per this interval.

<sup>9</sup>Of course, one can design different criteria for equivalence of the boxcar weighting function and  $w(t)$ . In our example we were simply looking for the width parameter of  $w(t)$  which would allow us to interpret the rate measurements with this function as ‘a number of events per time interval  $T$ ’.

One of the obvious shortcomings of boxcar averaging is that it does not allow meaningful differentiation of counting rates, while knowledge of time derivatives of the event occurrence rate is important for all physical models where such rate is a time-dependent parameter. Indeed, the time derivative of the rate measured with a boxcar function of width  $T$  is simply  $T^{-1}$  times the difference between the ‘original’ instantaneous pulse train and this pulse train delayed by  $T$ , and such representation of the rate derivative hardly provides physical insights. On the other hand, the time derivative of the ‘cascaded integrators’ weighting function  $w_n$  given by Eq. (13) is the bipolar pulse  $\dot{w}_n = \tau^{-1}(w_{n-1} - w_n)$ , and thus the time derivative of the rate evaluated with  $w_n(t)$  is a measure of the ‘disbalance’ of the rates within the moving window (positive for a ‘front-loaded’ sample, and negative otherwise).

#### 4. Measuring conditional rates and crossing rates for vector signals

It is often desirable to measure the counting rates satisfying a certain condition. For example, Eq. (3) computes the upward and downward threshold crossing rates, separately, by imposing the condition on the sign of the first time derivative of the signal at the intersection with the threshold. Such *conditional* rates are best considered through an extension to crossing rates of multicomponent (vector) signals.

Let us generalize the definition of threshold crossing rates for such multicomponent signals. For instance, a signal can be a two-dimensional vector composed of the original signal and its first time derivative. Then, for example, we can impose a condition on the rates by counting only the crossings at a certain speed (slope). That is, we want to measure the rate of crossings of  $\mathbf{x} = (x, \dot{x})$  with the threshold  $\mathbf{D} = (D_x, D_{\dot{x}})$ . The expression for such a rate can be written as

$$\begin{aligned} \mathcal{R}(D_x, D_{\dot{x}}, t) = & w * (\sqrt{(\dot{x} \Delta D_{\dot{x}})^2 + (\ddot{x} \Delta D_x)^2} \\ & \times f_{\Delta D} \{ \sqrt{[(D_x - x) \Delta D_{\dot{x}}]^2 + [(D_{\dot{x}} - \dot{x}) \Delta D_x]^2} \}) \end{aligned} \quad (14)$$

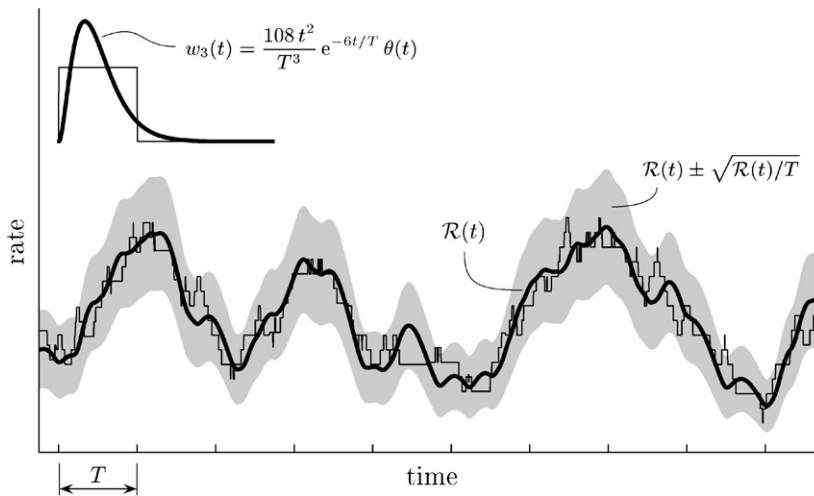


Fig. 7. Comparison of the rates measured with the boxcar (thin solid line) and the ‘triple-integrator’ test function ( $n = 3$  in Eq. (13), thick line) with  $\tau = T/6$ . The respective test functions are shown in the upper left corner of the figure.

where the width parameter of the probe is  $\Delta D = \Delta D_x \Delta D_{\dot{x}}$ . Obviously, an important special case  $D_{\dot{x}} = 0$  is the rate of occurrence of stationary points (both extrema and inflection points) at the threshold  $D$ , and the rates of occurrence of maxima (+) and minima (−), separately, are obtained by employing the factor  $\theta(\mp \ddot{x})$  in the right-hand side of Eq. (14), in a manner similar to Eq. (3).

The derivatives of the signal can be obtained by traditional techniques—for example, by means of RC differentiators or delay lines. In most instances, however, these derivatives can be evaluated without unnecessary modification of the signal in a fashion described in Section 2. For instance, assume that  $x(t)$  is a result of passing some signal from a sensor through an acquisition system with linear response, and that two components of this system have transient characteristics well described by  $H_\tau = \theta(t)(1 - e^{-t/\tau})$ . Each element with the transient characteristic  $H_\tau$  allows us to express the time derivative  $\dot{x}(t)$  of the signal through a simple difference between  $x(t)$  and the signal  $x_1(t)$  acquired *without* this element in the acquisition system (i.e.,  $x_1(t)$  bypasses this element in the system).

For example, the relationship among the three signals  $x(t)$ ,  $x_1(t)$ , and  $x_2(t)$  in the circuit shown in Fig. 2 is

$$x(t) = h_{\tau_1}(t) * x_1(t) = h_{\tau_1}(t) * h_{\tau_2}(t) * x_2(t). \quad (15)$$

Then, employing Eq. (6), the first and second time derivatives of the signal  $x(t)$  can be written as

$$\dot{x}(t) = \frac{1}{\tau_1} [x_1(t) - x(t)] \quad (16)$$

and

$$\ddot{x}(t) = \frac{1}{\tau_1 \tau_2} [x_2(t) - 2x_1(t) + x(t)] \quad (17)$$

respectively. Thus, a typical signal amplifier can output the signal along with its first two time derivatives, and Eqs. (16) and (17) can be utilized for a practical implementation of Eq. (14).

Fig. 8 illustrates usage of Eq. (14) for counting stationary points in a signal. Panel (a) of the figure shows the fragment of the signal in the interval  $[0, T]$ . The thresholds at which the stationary points occur are shown by the dashed lines. Panel (b) of the figure shows the number of stationary points in this time interval, as a function of threshold, computed according to Eq. (14). Note that the fragment of the signal shown contains ‘incomplete’ crossings of the threshold  $D = (0, 0)$ , and thus the total number of counts at  $D_x = 0$  is 7.5 stationary points.

The relation of the mathematical formalism expressed by Eq. (14) to real physical devices might be somewhat obscure. In order to illustrate such a relation, let us employ a conventional

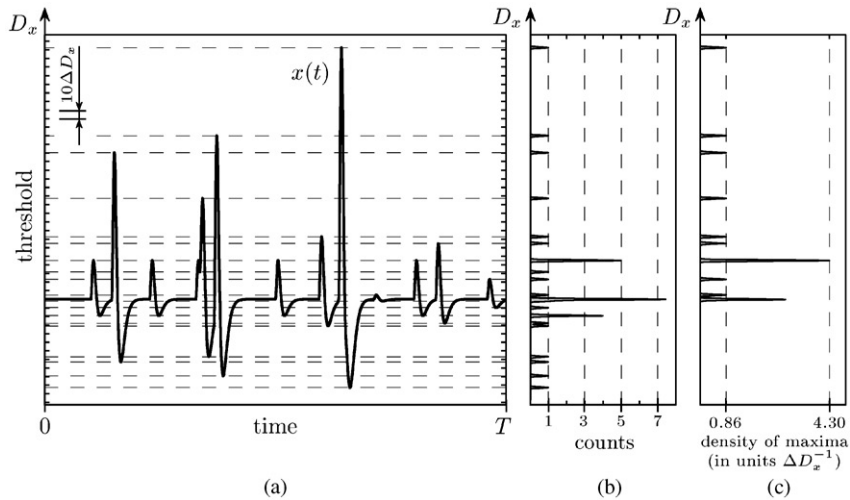


Fig. 8. Counting stationary points and maxima in a signal by means of Eqs. (14) and (19). Panel (a): Fragment of the signal in the interval  $[0, T]$ . Panel (b): Number of stationary points as a function of threshold. Panel (c): Density of maxima.

analog oscilloscope for measuring the (time-dependent) rates of occurrence of stationary points in some signal  $x(t)$ . As shown in Fig. 9, a voltage proportional to  $x(t)$  is fed to the horizontal deflecting plates, and a voltage proportional to  $\dot{x}(t)$  to the vertical plates. When both  $X$  and  $Y$  inputs are constant, the electron beam produces a static spot on the screen. In all real oscilloscopes, this spot would have a finite size, and its shape and brightness can be adjusted. Without loss of generality, we can assume that the brightness of the spot is uniform, and it is an ellipse with the semiaxes  $\Delta D_x$  and  $\Delta D_{\dot{x}}$ . If we modulate the intensity of the electron beam by  $Z(t) = \sqrt{(\dot{x} \Delta D_{\dot{x}})^2 + (\ddot{x} \Delta D_x)^2}$ , then the brightness of the projected spot will be proportional to the speed of the movement of this spot across the screen. If the afterglow half-time of the screen's luminophor is  $T_{1/2} = \tau \ln 2$ , then the brightness of the displayed picture on the screen at  $(D_x, D_{\dot{x}})$  will be described by  $\mathcal{R}(D_x, D_{\dot{x}}, t)$  given by Eq. (14), where

$$f_{\Delta D}(y) = \frac{1}{\pi \Delta D_x \Delta D_{\dot{x}}} \times [\theta(y + \Delta D_x \Delta D_{\dot{x}}) - \theta(y - \Delta D_x \Delta D_{\dot{x}})] \quad (18)$$

and the time averaging window is  $w(t) = h_\tau(t)$ ,  $\tau = T_{1/2}/\ln 2$ . By measuring the brightness at the

horizontal axis  $D_{\dot{x}} = 0$ , we will effectively measure the rate of occurrence of the stationary points of  $x(t)$ . As can be seen from Fig. 9, this brightness corresponds to the counts measured in the example of Fig. 8(b).

A large variety of signal characteristics can be described in a manner similar to Eqs. (10) and (14). For example, the *density of maxima* in a signal can be written as

$$\phi_+(D, t) = \frac{w(t) * \{K(t) f_{\Delta D_x}[D - x(t)]\}}{w(t) * K(t)} \quad (19)$$

where

$$K(t) = \ddot{x}(t) \theta[-\ddot{x}(t)] f_{\Delta D_{\dot{x}}}[-\dot{x}(t)] \quad (20)$$

and a stationary inflection point is counted as a half of a maximum.<sup>10</sup> Obviously, Eq. (19) thus describes a *pulse-height analyzer*. Panel (c) of Fig. 8 shows the density of maxima, computed using Eq. (19), for the signal shown in Panel (a).

To conclude this section, let us point out that the threshold density given by Eq. (19) can be

<sup>10</sup>Note that Eq. (19) with  $K(t)$  given by Eq. (20) expresses the *fraction of the total number of maxima at threshold  $D$  per (infinitesimally small) threshold interval  $dD$* , and thus it is the density of maxima. Indeed, the numerator of Eq. (19) is the number of maxima at  $D$  per interval  $dD$ . The denominator, on the other hand, is just the total number of maxima since it is the integral of the numerator over all thresholds.

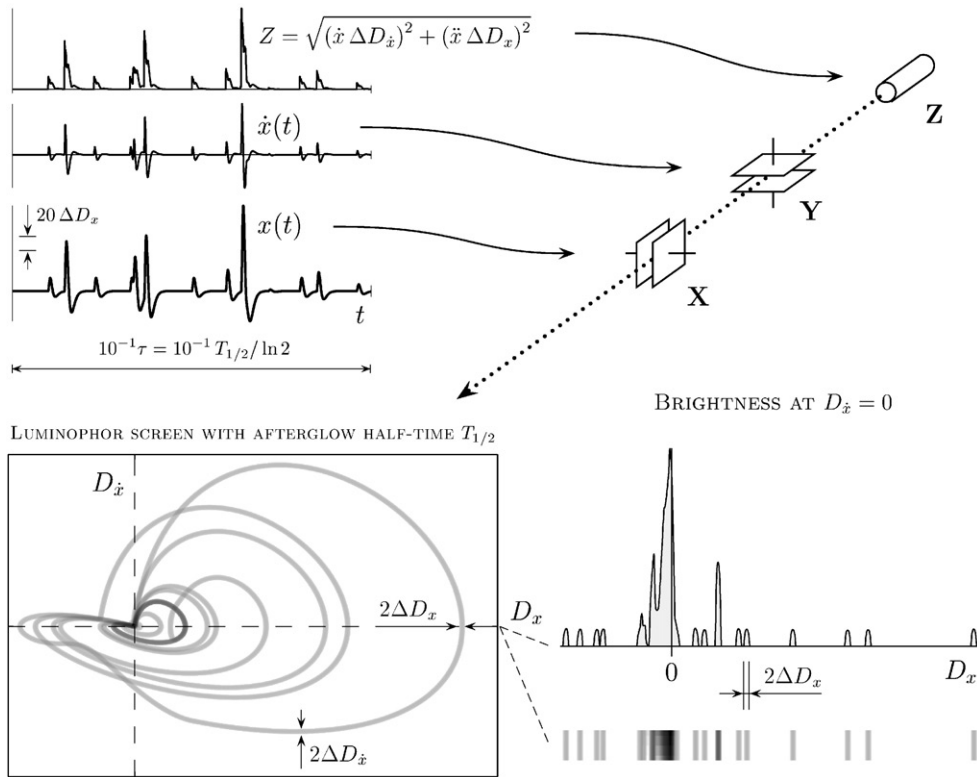


Fig. 9. Using conventional analog oscilloscope for counting stationary points in a signal.

viewed as a particular appearance of a general *modulated threshold density*

$$\phi(D, t) = \frac{w(t) * \{K(t) f_{\Delta D}[D - x(t)]\}}{w(t) * K(t)} \quad (21)$$

where  $K(t)$  is a unipolar *modulating signal*. Various choices of the modulating signal allow us to introduce different types of threshold densities and impose different conditions on these densities. For example, the simple *amplitude density* is given by the choice  $K(t) = \text{const.}$ , and setting  $K(t) = |\dot{x}(t)|$  leads to the *counting density*.

### 5. Conclusion

Physical measurements often require characterization of rates of occurrence of various coincidence events—for example, instances of crossings of a signal with a given threshold, or occurrence of extrema of a certain amplitude. The approach

described in this paper enables simple and efficient implementation of various counting systems in robust analog devices, which we call *multivariate counting analyzers*. The rates measured by such counters can be simple or conditional rates for scalar as well as for multicomponent (vector) signals. These analyzers can be easily implemented in discrete or integrated electronic circuits, do not suffer from dead time effects, allow substantial reduction of pileup effects, and have other significant advantages with respect to the existing counting devices. For example, in space applications the analog approach has an outstanding advantage of the absence of any requirement for software or firmware, which eliminates any potential for disaster caused by unforeseen ‘bugs’ in the code. The proposed counters would be well suited for operation in autonomous conditions such as mobile communication, space missions, prosthetic devices, etc. In addition, the analog output of these analyzers can be used as a feedback signal in various control systems, e.g.

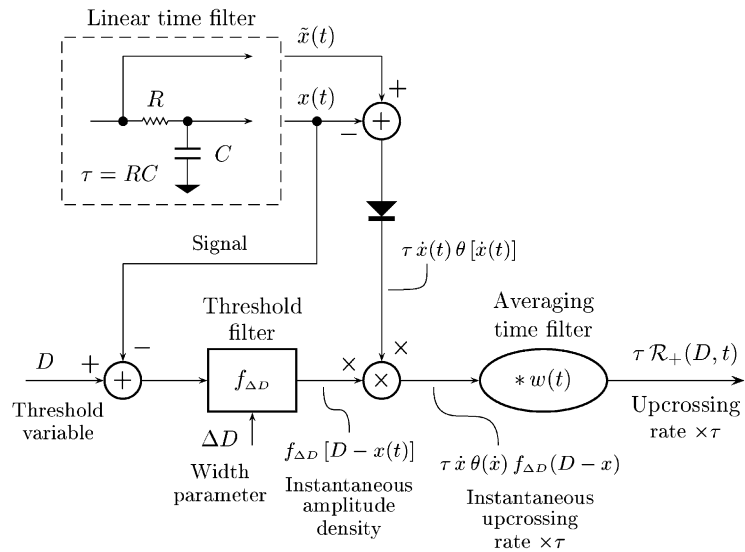


Fig. 10. Simplified schematic of a positive slope threshold crossing counter.

cardiac pacemakers. This feedback can also be used for adaptation of the parameters of the acquisition system for the optimal compromise between the amplitude and the time resolution, and for reduction of the effects caused by noise.

Let us use the example of a *positive slope threshold crossing counter* to reiterate the main principles of our approach to the counting problem. A simplified schematic of such a counter is shown in Fig. 10.

In general terms, we can view a device accomplishing some particular signal processing task as a sequence of (linear) *time filters* and *threshold filters*. These filters are connected in such a fashion that their inputs and outputs can be represented by algebraic expressions comprising these inputs and outputs. For example, the input of the second (averaging) time filter in Fig. 10,  $\tau \dot{x} \theta(\dot{x}) f_{\Delta D}(D - x)$ , is the product of the threshold-filtered first output of the first time filter (the signal  $x(t)$ ) and the positive value of the difference between the second ( $\tilde{x}$ ) and first ( $x$ ) outputs of the first time filter,  $(\tilde{x} - x)\theta(\tilde{x} - x)$ . The output of the second time filter  $\tau \mathcal{R}_+$  then represents  $\tau$  times the rate of upcrossings of the threshold  $D$  by the signal  $x(t)$  in the moving time window  $w$  (i.e.,  $\mathcal{R}_+(D, t) = w(t) * \{\dot{x}(t) \theta[\dot{x}(t)] f_{\Delta D}[D - x(t)]\}$ ).

Knowledge of various derivatives of the event occurrence rate is important for all physical

models where such rate is a variable. Since in the counting analyzers described in this article both the time and threshold averaging of the instantaneous rates are performed by continuous kernels, these analyzers enable meaningful direct measurements of such derivatives. Thus continuous rates and densities can enter partial differential equations used in various control systems.

The analyzers described here also enable direct measurements of *multivariate* distributions, i.e., distributions in which the threshold argument is a vector. For example, an energy-pitch angle distribution of charged particles in the Earth magnetosphere can be directly measured by an instrument on board a spacecraft, without the necessity of complicated ground data analysis.

Further advantages of the analog method described above include the capability to extend the dynamic range in counting rate of event detecting systems. For example, a wide dynamic range is essential for space radiation measurements, where instruments are often carried through radiation environments that vary by many orders of magnitude in intensity—factors of a billion are typical [16–19]. Signals resulting from sensors exposed to such environments have complicated variations related to the frequencies and sizes of events. The process of achieving the

goals of measurement and observation, namely, determining the frequencies and event sizes, is highly constrained by the available mass, power, volume, and information transmission bandwidth. From the limited amounts of mass, power, volume, and information rate, claims for various instruments must be met. The approach to measurements described here has the ability to improve significantly over digital counting—specifically to be simpler, lighter, smaller, less expensive, more robust and accurate—has a larger dynamic range of event amplitudes and frequencies for given instrument power, and to be more adaptable. Since breakthroughs often occur when measurements and observations are made more sensitive, robust, and capable, further exploration and exploitation of the analog counting is likely to be important.

## Acknowledgements

We would like to express our deepest gratitude to Quentin Bristow of the Geological Survey of Canada for extensive discussion and numerous suggestions regarding various aspects of our presentation. His invaluable contribution has helped us to greatly improve the clarity and readability of the manuscript. 12pt >

## Appendix A. Formal expression for threshold crossing rates

Let us demonstrate that Eq. (1) indeed expresses the rate of crossings of the threshold  $D$  by a continuous signal  $x(t)$  in the time interval  $0 \leq t \leq T$ . This equation can be re-written in an extended form as

$$\begin{aligned}
 T\mathcal{R}(D) &= \int_0^T dt |\dot{x}(t)| \delta[D - x(t)] \\
 &= \int_0^T dt |\dot{x}(t)| \sum_i \frac{\delta(t - t_i)}{|\dot{x}(t_i)|} \\
 &= \int_0^T dt \sum_i \frac{|\dot{x}(t_i)| \delta(t - t_i)}{|\dot{x}(t_i)|} \\
 &= \sum_i \int_0^T dt \delta(t - t_i) \quad (\text{A.1})
 \end{aligned}$$

where the sum goes over all  $t_i$  such that  $x(t_i) = D$ . Thus  $T\mathcal{R}(D)$  is the total number of crossings in the time interval  $0 \leq t \leq T$  and  $\mathcal{R}(D)$  is the rate of such crossings.

In Eq. (A.1) we have used the following property of the Dirac  $\delta$ -function (see [20, p. 610, Eq. (A15)], for example):

$$\delta[a - f(x)] = \sum_i \frac{\delta(x - x_i)}{|f'(x_i)|} \quad (\text{A.2})$$

where  $|f'(x_i)|$  is the absolute value of the derivative of  $f(x)$  at  $x_i$ , and the sum goes over all  $x_i$  such that  $f(x_i) = a$ . We have also used the fact that (see [14, p. 60, Eq. (11)], for example)

$$f(x)\delta(x - a) = f(a)\delta(x - a). \quad (\text{A.3})$$

## References

- [1] A.V. Nikitin, Pulse pileup effects in counting detectors, Ph.D. Thesis, University of Kansas, Lawrence, 1998.
- [2] A.V. Nikitin, R.L. Davidchack, T.P. Armstrong, Nucl. Instr. and Meth. A 411 (1998) 159.
- [3] H.F. Freundlich, E.P. Hincks, W.J. Dzeroff, Rev. Sci. Inst. 18 (1947) 90.
- [4] C.H. Westcott, G.C. Hanna, Rev. Sci. Inst. 20 (1949) 181–188.
- [5] E. Fairstein, J. Hahn, Nucleonics 23 (7) (1965) 56–61; E. Fairstein, J. Hahn, Nucleonics 23 (9) (1965) 81; E. Fairstein, J. Hahn, Nucleonics 23 (11) (1965) 50; E. Fairstein, J. Hahn, Nucleonics 24 (1) (1966) 54; E. Fairstein, J. Hahn, Nucleonics 24 (3) (1966) 68.
- [6] S.A. Gary, Effect of filtering on noise and timing in nuclear particle detection, Technical Memorandum TG 1136, Johns Hopkins University, APL, Silver Spring, MD, 1970.
- [7] D.W. Datlowe, Nucl. Instr. and Meth. 145 (1977) 365.
- [8] Q. Bristow, R.G. Harrison, Nucl. Geophys. 5 (1991) 141.
- [9] B. Sabbah, I. Klein, A. Arbel, Nucl. Instr. and Meth. 95 (1971) 163.
- [10] R. Pepelnik, G.P. Westphal, B. Anders, Nucl. Instr. and Meth. 226 (1984) 411.
- [11] G.P. Westphal, Nucl. Instr. and Meth. B 10/11 (1985) 1047.
- [12] A. Chalupka, S., Tagesen, Nucl. Instr. and Meth. A 245 (1986) 159–161.
- [13] V.R. Drndarevic, P. Ryge, T. Gozani, IEEE Trans. Nucl. Sci. NS-36 (1) (1989) 1326.
- [14] P.A.M. Dirac, The Principles of Quantum Mechanics, 4th Edition, Oxford University Press, London, 1958.
- [15] A.V. Nikitin, R.L. Davidchack, Proc. Roy. Soc. London A (2002), in press.

- [16] E.T. Saris, S.M. Krimigis, T.P. Armstrong, J. Geophys. Res. 81 (1976) 2341.
- [17] D.J. Williams, The ion–electron magnetic separation and solid state detector detection system flown on IMP 7 and 8:  $E_p \geq 50$  keV,  $E_e \geq 30$  keV, Technical Report ERL 393-SEL 40, NOAA, 1977.
- [18] S.M. Krimigis, T.P. Armstrong, W.I. Axford, C.O. Bostrom, C.Y. Fan, G. Gloeckler, L.J. Lanzerotti, Space Sci. Rev. 21 (1977) 329.
- [19] L.J. Lanzerotti, R.E. Gold, K.A. Anderson, T.P. Armstrong, R.P. Lin, S.M. Krimigis, M. Pick, E.C. Roelof, E.T. Sarris, G.M. Simnett, W.E. Frain, Astron. Astrophys. 92 (Suppl.) (1992) 349.
- [20] A.S. Davydov, Quantum Mechanics, International Series in Natural Philosophy, 2nd Edition, Pergamon Press, Oxford, 1988 (2nd Russian Edition published by Nauka, Moscow, 1973).